

Effects of anisotropy in an anisotropic extension of w CDM model

Vikrant Yadav,^{1,*} Santosh Kumar Yadav,^{2,†} and Rajpal^{1,‡}

¹*School of Basic and Applied Sciences, Raffles University, Neemrana - 301705, Rajasthan, India*

²*School of CS & AI, SR University, Warangal-506371, Telangana, India*

In this paper, we derive observational constraints on an anisotropic w CDM model from observational data including Baryonic Acoustic Oscillations (BAOs), Cosmic Chronometer (CC), Big Bang Nucleosynthesis (BBN), Pantheon Plus (PP) compilation of Type Ia supernovae, and SH0ES Cepheid host distance anchors. We find that anisotropy is of the order 10^{-13} , and its presence in the w CDM model reduces H_0 tension by $\sim 2\sigma$ and $\sim 1\sigma$ in the analyses with BAO+CC+BBN+PP and BAO+CC+BBN+PPSH0ES data combinations, respectively. In both analyses, the quintessence form of dark energy is favored at 95% CL.

I. INTRODUCTION

Our Universe is expanding with accelerated rate of expansion as observed from type Ia supernovae (SNe Ia) observations [1, 2]. Later on, various other observations such as the large scale structure (LSS), the Baryonic Acoustic Oscillations (BAOs) and the cosmic microwave background (CMB) supported this observation. A number of cosmological models have been proposed/investigated in the literature to help us comprehend the dynamics of the universe. But, among all cosmological models, Λ CDM has proven to be the simplest mathematical model which has widely been accepted by the cosmological community and referred to as the standard cosmological model of cosmology. Basically, this model is composed of two main parts: cold (non-relativistic) dark matter (CDM) which is the reason behind the structure formation, and dark energy (DE) in the form of cosmological constant (Λ) which causes the late time accelerated expansion of Universe. The Λ CDM model provides an excellent fit across a broad range of scales and epochs [3–7], and successfully describes late-time accelerated expansion of the Universe [8, 9]. Despite the excellent fit to the current available cosmological observations, the model faces several theoretical and observational challenges. For instance, the nature of DE is not known accurately so far, and within the Λ CDM paradigm, DE is regarded as the cosmological constant in its most basic form, lacking any solid physical foundation. Except for its typical gravitational interactions with other components, the exact nature of dark matter remains unknown. Also, there is no concrete explanation of ‘coincidence problem’ stating why, despite having very distinct cosmic evolutions, do the dark matter densities and the DE have the same order? Is this coincidence indicating the possibility for interaction between the dark sector components? Up to what extent the cosmological principle has been tested? Is the Universe homogeneous and isotropic at cosmic scales?

Further, a few indications in the observations point towards the need to expand the Λ CDM model in order to account for the growing conflicts between measurements made at early (high redshifts) and late (low redshifts) Universe [10, 11]. The Hubble constant, H_0 , which represents the Universe’s current rate of expansion, has the greatest statistically significant tension. The Hubble tension appears when we compare the value of H_0 predicted by CMB measurements within the Λ CDM framework and the direct local distance ladder measurements, that is, the one estimated by the Cepheid calibrated supernovae SNe Ia. In particular, the Hubble tension is referred to as the disagreement at 5σ between the latest SH0ES (Supernovae and H_0 for the equation of state (EoS) of DE) collaboration [12] constraint, $H_0^{\text{R}22} = (73.04 \pm 1.04) \text{ km s}^{-1} \text{ Mpc}^{-1}$ at 68% confidence level (CL), based on the supernovae calibrated by Cepheids, and the *Planck* collaboration [3] value, $H_0 = (67.27 \pm 0.60) \text{ km s}^{-1} \text{ Mpc}^{-1}$ at 68% CL. The Hubble tension may be defined as a difference between the observed value of H_0 from two sets of observations: (i) all of the direct late time Λ CDM independent measurements, and (ii) all of the indirect model dependent estimations at early times. In general, the value of H_0 obtained at late times is greater than the one obtained at early times.

This disparity could indicate the existence of novel physics outside of the Λ CDM cosmology [13–18]. In the literature, a number of extensions of Λ CDM have been suggested to resolve the H_0 tension. These extensions include but not limited to: DM-DE interactions [19–25]; decaying DM [26–29]; introducing Early DE [30–34]; and introducing a sign-switching DE at intermediate redshifts ($z \sim 2$) [35–39]. The current status on H_0 tension and possible solutions can be found in recent review articles [40–43].

The Cosmological Principle (CP), which asserts that the Universe is statistically homogenous and isotropic in space and matter on vast scales (100Mpc), is one of the fundamental tenets of Λ CDM cosmology. Mathematically, such a universe is described by the Friedmann-Lemaître-Robertson-Walker (FLRW) space-time metric, in which all three of the metric’s spatial orthogonal components are functions of cosmic time (t) exclusively. This is the primary space-time metric that facilitates the cre-

* vikuyd@gmail.com

† sky91bbaulko@gmail.com

‡ rajpal05041985@gmail.com

ation of the effective and remarkably predictive standard model of cosmology. However, observational data suggest that there are slight fluctuations in CMB intensities originating from various directions of sky [44]. Gamma Ray Bursts (GRBs), Quasars, Galaxies, and SNe Ia are among the recent findings that suggest the Universe may be anisotropic and provide substantial observational evidence (see [45] and references therein). There are other interesting observational evidences, which have questioned the validity of CP, for instance, a strong evidence for a violation of the CP of isotropy is found by the authors in [46] after analysing the Planck Legacy temperature anisotropy data. This violation is likely to represent a statistical fluctuation of order $\sim 10^{-9}$. Also, see the recent and interesting review [47] where the authors emphasise differences and synergies that truly stimulate additional research in this field as they detail existing observational clues for departures from the predictions of CP. The spatially homogeneous and anisotropic Universe is expressed mathematically by homogeneous and anisotropic metrics and corresponding models are commonly known as Bianchi type models [48, 49]. The simplest of the various Bianchi type models is the Bianchi type I model. The empirical limitations on the Bianchi type I model might offer a platform for evaluating the precision of FLRW models characterising the current era of the universe. Various anisotropic generalizations of the standard Λ CDM model have been investigated in recent years. In [50], the authors analyze an anisotropic model with the CMB and BAO data by fixing the drag redshift as $z_d = 1059.6$ and the last scattering redshift as $z_* = 1089.9$ and constrain the anisotropy parameter, $\Omega_{\sigma 0} \lesssim 10^{-15}$. A similar investigation is done in [51] by considering anisotropic expansion and curvature together from different data sets and discovered very little present-day expansion anisotropy. Other anisotropic models are also investigated by using different observational data in different contexts, see [52–58]. In [59], a theoretical approach of spatially homogeneous universes with late-time anisotropy is discussed. Most recently, in [60] an anisotropic model, Λ CDM + $\Omega_{\sigma 0}$ is investigated with the aim to derive CMB independent constraints on H_0 with BAO, BBN, CC, Pantheon Plus and SH0ES data. Following [60], we are motivated here to derive observational constraints on two simplest extensions of vanilla Λ CDM model: (i) an isotropic extension by taking a constant EoS of DE instead of cosmological constant, namely w CDM model; (ii) an anisotropic extension, namely w CDM + $\Omega_{\sigma 0}$ by adding expansion anisotropy to w CDM model. It is well known that the nature of DE could be investigated through its EoS parameter. As stated above, the fundamental nature of DE is unknown and there is no strong physical basis for assuming DE in the form of cosmological constant whose density remains constant even in an expanding background. In this paper, we have assumed a constant EoS parameter of DE. Our primary goal in this work is to analyze the possible effects of anisotropy on the constant

EoS parameter of DE and the Hubble constant H_0 . For this, we derive observational constraints using the recent observational data and compare the results of w CDM and w CDM + $\Omega_{\sigma 0}$ models with the results obtained in [60] for Λ CDM and Λ CDM + $\Omega_{\sigma 0}$, respectively.

The structure of the paper is as follows: In Section II, we describe the details of the considered models. In Section III, we provide a brief overview of the data sets and methodology used for the observational analysis of the models. In Section IV, we present the observational constraints on the models, and discuss the results. In Section V, we conclude with the main findings of our study.

II. GOVERNING EQUATIONS AND MODELS

We investigate an extension of FLRW spacetime, the Bianchi type I metric, with three orthogonal directions of different scale factors, given by

$$ds^2 = -dt^2 + A^2 dx^2 + B^2 dy^2 + C^2 dz^2, \quad (1)$$

where A, B , and C are functions of cosmic time t only and represent the scale factors along the principal axes x, y and z , respectively. Further, we define the average expansion scale factor: $a = (ABC)^{\frac{1}{3}}$, and the average Hubble parameter: $H = \frac{\dot{a}}{a} = \frac{(H_x + H_y + H_z)}{3}$, where the corresponding directional Hubble parameters along the principal axes x, y , and z are being defined as $H_x = \frac{\dot{A}}{A}$, $H_y = \frac{\dot{B}}{B}$, and $H_z = \frac{\dot{C}}{C}$ respectively.

The Einstein field equations in GR read as

$$G_{\mu\nu} \equiv R_{\mu\nu} - \frac{1}{2}g_{\mu\nu}R = 8\pi GT_{\mu\nu}, \quad (2)$$

where the left side of the above expression shows the Einstein tensor $G_{\mu\nu}$, the Ricci tensor $R_{\mu\nu}$, the Ricci scalar R , and the metric tensor $g_{\mu\nu}$. Additionally, the right side shows the Newton's gravitational constant G and the energy momentum tensor $T_{\mu\nu}$. Further, for a perfect fluid with energy density ρ and pressure p , $T_{\mu\nu}$ takes the form

$$T_{\mu}^{\nu} = \text{diag}[-\rho, p, p, p]. \quad (3)$$

As a result of the twice-contracted Bianchi identity ($G^{\mu\nu}_{;\nu} = 0$), the Einstein field equations (2) satisfy the conservation equation

$$T^{\mu\nu}_{;\nu} = 0. \quad (4)$$

In case of the perfect fluid matter distribution, it reduces to

$$\dot{\rho} + 3H(\rho + p) = 0, \quad (5)$$

where the dot denotes its cosmic time(t) derivative. The evolution of the energy density ρ_i of a perfect fluid i with pressure p_i , energy density ρ_i , and constant EoS

$w_i = p_i/\rho_i$ is provided by the continuity equation (5), which is as follows:

$$\rho_i = \rho_{i0} a^{-3(1+w_i)}, \quad (6)$$

where ρ_{i0} stands for the current value of ρ_i , that is, at $a = a_0 = 1$. Here, $a = a_0 = 1$ signifies the present day value of the cosmic scale factor a . From this point on, every quantity with the subscript 0 indicates its value in the present day universe. We consider that the universe is made up of the standard cosmic fluids, namely the radiation (photons and neutrinos) whose EoS is $w_r = p_r/\rho_r = \frac{1}{3}$, pressureless fluid (baryonic and cold dark matter) whose EoS is $w_m = p_m/\rho_m = 0$, and DE fluid with a constant EoS w_{de} , to be fixed by observations in the analysis. Further, assuming only gravitational interaction between these energy components, the continuity equation (5) being satisfied by each component separately, and in view of (6), this gives

$$\rho \equiv \rho_r + \rho_m + \rho_{de} = \rho_{r0} a^{-4} + \rho_{m0} a^{-3} + \rho_{de0} a^{-3(1+w_{de0})} \quad (7)$$

Further, for the Bianchi type I metric (1), the Einstein field equations (2) result into to the following set of differential equations:

$$\frac{\dot{A}\dot{B}}{AB} + \frac{\dot{B}\dot{C}}{BC} + \frac{\dot{A}\dot{C}}{AC} = 8\pi G\rho, \quad (8)$$

$$-\frac{\ddot{B}}{B} - \frac{\ddot{C}}{C} - \frac{\dot{B}\dot{C}}{BC} = 8\pi Gp, \quad (9)$$

$$-\frac{\ddot{A}}{A} - \frac{\ddot{C}}{C} - \frac{\dot{A}\dot{C}}{AC} = 8\pi Gp, \quad (10)$$

$$-\frac{\ddot{A}}{A} - \frac{\ddot{B}}{B} - \frac{\dot{A}\dot{B}}{AB} = 8\pi Gp. \quad (11)$$

The shear scalar may be expressed as follows in terms of the directional Hubble parameters:

$$\sigma^2 = \frac{(H_x - H_y)^2 + (H_y - H_z)^2 + (H_z - H_x)^2}{6}. \quad (12)$$

The equations (8)-(11) can be recast as follows:

$$3H^2 - \sigma^2 = 8\pi G\rho, \quad (13)$$

$$\dot{H}_x - \dot{H}_y + 3H(H_x - H_y) = 0, \quad (14)$$

$$\dot{H}_y - \dot{H}_z + 3H(H_y - H_z) = 0, \quad (15)$$

$$\dot{H}_z - \dot{H}_x + 3H(H_z - H_x) = 0. \quad (16)$$

We derive the following shear propagation equation using these equations (14)-(16) and the time derivative of σ^2 provided in Eq. (12):

$$\dot{\sigma} + 3H\sigma = 0. \quad (17)$$

Its integration further leads to

$$\sigma^2 = \sigma_0^2 a^{-6}. \quad (18)$$

Using equations (7) and (18) into (13), we obtain

$$\frac{H^2}{H_0^2} = \Omega_{\sigma 0} a^{-6} + \Omega_{r0} a^{-4} + \Omega_{m0} a^{-3} + \Omega_{de0} a^{-3(1+w_{de0})}, \quad (19)$$

where $\Omega_{\sigma 0} = \frac{\sigma_0^2}{3H_0^2}$, $\Omega_{r0} = \frac{8\pi G}{3H_0^2} \rho_{r0}$, $\Omega_{m0} = \frac{8\pi G}{3H_0^2} \rho_{m0}$ and $\Omega_{de0} = \frac{8\pi G}{3H_0^2} \rho_{de0}$, respectively denote the expansion anisotropy, radiation, matter, and DE density parameters, satisfying $\Omega_{\sigma 0} + \Omega_{r0} + \Omega_{m0} + \Omega_{de0} = 1$. Here, the expansion anisotropy parameter $\Omega_{\sigma 0}$ is purely a geometric term which is non-negative.

Furthermore, the generalized Friedmann equation (19) depicts the spatially flat and homogeneous but probably non-isotropic Universe (because of the presence of the expansion anisotropy). We denote this model by w CDM+ $\Omega_{\sigma 0}$ and the set of free baseline parameters for this model is given by

$$\mathcal{P}_{w\text{CDM}+\Omega_{\sigma 0}} = \{\omega_b, \omega_c, H_0, \Omega_{\sigma 0}, w_{de0}\}.$$

Here $\omega_b = \Omega_b h^2$ and $\omega_c = \Omega_c h^2$ are physical density parameters of baryons and CDM, respectively, in the present Universe, H_0 is the Hubble constant and $\Omega_{\sigma 0}$ is the expansion anisotropy parameter.

In the absence of expansion anisotropy, equation (19) reduces to

$$\frac{H^2}{H_0^2} = \Omega_{r0} a^{-4} + \Omega_{m0} a^{-3} + \Omega_{de0} a^{-3(1+w_{de0})}. \quad (20)$$

It is an isotropic extension of Λ CDM cosmology. We denote this model by w CDM and the set of free baseline parameters for this model is given by

$$\mathcal{P}_{w\text{CDM}} = \{\omega_b, \omega_c, H_0, w_{de0}\}.$$

We follow standard neutrino scheme with normal hierarchy which has three species of neutrino, out of which two are massless and one is massive neutrino with the standard number of effective neutrino species, $N_{\text{eff}} = 3.046$ and minimum allowed mass, $m_\nu = 0.06$ eV.

III. DATA AND METHODOLOGY

The following data sets have been used in this work:

Baryon Acoustic Oscillation (BAO): Updates on BAO measurements utilising galaxies, quasars, and Lyman- α ($\text{Ly}\alpha$) for completed experiments are provided by the Sloan Digital Sky Survey (SDSS) [61]. These experiments involve the compilation of data from BOSS, eBOSS, SDSS, and SDSS-II, making accessible, as indicated in Table I, independent BAO measurements of angular-diameter distances and Hubble distances relative to the sound horizon from eight separate samples.

At the drag redshift (z_d), the comoving size of the sound horizon (r_s) is r_d , and it is given by

$$r_d = r_s(z_d) = \int_{z_d}^{\infty} \frac{c_s dz}{H(z)}, \quad (21)$$

where $c_s = \frac{c}{\sqrt{3(1+\mathcal{R})}}$ is the sound speed of the baryon-photon fluid; $\mathcal{R} = \frac{3\Omega_{b0}}{4\Omega_{\gamma0}(1+z)}$ with $\Omega_{b0} = 0.022h^{-2}$ being the present-day physical density of baryons and $\Omega_{\gamma0} = 2.469 \times 10^{-5}h^{-2}$ being the present-day physical density of photons [62, 63].

Direct constraints on the values $D_H(z)/r_d$ and $D_M(z)/r_d$ are provided by the BAO measurements. We calculate the Hubble distance as follows:

$$D_H(z) = \frac{c}{H(z)}. \quad (22)$$

For flat cosmology, we calculate the comoving angular diameter distance ($D_M(z)$) as follows:

$$D_M(z) = \frac{c}{H_0} \int_0^z dz' \frac{H_0}{H(z')}. \quad (23)$$

The spherically averaged distance ($D_V(z)$) is defined as follows:

$$D_V(z) \equiv [zD_M^2(z)D_H(z)]^{1/3}. \quad (24)$$

We have opted d_1 for $D_V(z)/r_d$, d_2 for $D_M(z)/r_d$, and d_3 for $D_H(z)/r_d$. Then, the chi-squared function for each measurement in Table I is written as follows:

$$\begin{aligned} \chi_{B_1}^2 &= \sum_{i=1}^2 \left(\frac{d_1^{\text{obs}}(z_i) - d_1^{\text{th}}(z_i)}{\sigma_{d_1^{\text{obs}}(z_i)}} \right)^2, \\ \chi_{B_2}^2 &= \sum_{j=1}^6 \left(\frac{d_2^{\text{obs}}(z_j) - d_2^{\text{th}}(z_j)}{\sigma_{d_2^{\text{obs}}(z_j)}} \right)^2, \\ \chi_{B_3}^2 &= \sum_{j=1}^6 \left(\frac{d_3^{\text{obs}}(z_j) - d_3^{\text{th}}(z_j)}{\sigma_{d_3^{\text{obs}}(z_j)}} \right)^2. \end{aligned} \quad (25)$$

Here, d^{obs} denotes the observed distance value as shown in Table I, whereas d^{th} denotes the theoretical value computed for the models under consideration. The effective redshifts for MGS and eBOSS ELG samples in the $D_V(z)/r_d$ scenario are denoted as z_i ($i = 1, 2$). For $D_M(z)/r_d$ and $D_H(z)/r_d$, the effective redshifts for the six measurements are labelled as z_j ($j = 1, 2, 3, 4, 5, 6$) which correspond to BOSS Galaxy, eBOSS Galaxy, eBOSS LRG, eBOSS Quasar, Ly α -Ly α , and Ly α -Quasar, respectively.

Table I. Clustering measurements for the BAOs from Ref. [61].

Parameter	z_{eff}	$D_V(z)/r_d$	$D_M(z)/r_d$	$D_H(z)/r_d$
MGS	0.15	4.47 ± 0.17	—	—
BOSS Galaxy	0.38	—	10.23 ± 0.17	25.00 ± 0.76
BOSS Galaxy	0.51	—	13.36 ± 0.21	22.33 ± 0.58
eBOSS LRG	0.70	—	17.86 ± 0.33	19.33 ± 0.53
eBOSS ELG	0.85	$18.33^{+0.57}_{-0.62}$	—	—
eBOSS Quasar	1.48	—	30.69 ± 0.80	13.26 ± 0.55
Ly α -Ly α	2.33	—	37.6 ± 1.9	8.93 ± 0.28
Ly α -Quasar	2.33	—	37.3 ± 1.7	9.08 ± 0.34

Table II. Compilation of CC measurements of $H(z)$.

z	$H(z)$	$\sigma_{H(z)}$	Ref.
0.07	69.0	19.6	[65]
0.09	69	12	[66]
0.12	68.6	26.2	[65]
0.17	83	8	[66]
0.179	75	4	[67]
0.199	75	5	[67]
0.20	72.9	29.6	[65]
0.27	77	14	[66]
0.28	88.8	36.6	[65]
0.352	83	14	[67]
0.38	83	13.5	[68]
0.4	95	17	[66]
0.4004	77	10.2	[68]
0.425	87.1	11.2	[68]
0.445	92.8	12.9	[68]
0.47	89.0	49.6	[69]
0.4783	80.9	9	[68]
0.48	97	62	[70]
0.593	104	13	[67]
0.68	92	8	[67]
0.75	98.8	33.6	[71]
0.781	105	12	[67]
0.8	113.1	15.1	[72]
0.875	125	17	[67]
0.88	90	40	[70]
0.9	117	23	[66]
1.037	154	20	[67]
1.3	168	17	[66]
1.363	160	33.6	[73]
1.43	177	18	[66]
1.53	140	14	[66]
1.75	202	40	[66]
1.965	186.5	50.4	[73]

For the BAO measurements, the cumulative chi-squared expression, denoted as χ_{BAO}^2 , is therefore formulated as follows:

$$\chi_{\text{BAO}}^2 = \chi_{B_1}^2 + \chi_{B_2}^2 + \chi_{B_3}^2. \quad (26)$$

Cosmic Chronometer (CC): The Cosmic Chronometer (CC) uses a reliable technique to monitor the universe's historical expansion through the analysis of $H(z)$ measurements. 33 $H(z)$ measurements from CC have been compiled, covering redshift values from 0.07 to 1.965. Table II provides a thorough description of these measurements and the corresponding references. The idea behind these measurements was first presented in [64], whereby a fundamental connection was established between the Hubble parameter $H(z)$, redshift z , and cosmic time t :

$$H(z) = -\frac{1}{1+z} \frac{dz}{dt}. \quad (27)$$

We formulate the chi-squared function χ_{CC}^2 associated

with these measurements as follows:

$$\chi_{\text{CC}}^2 = \sum_{i=1}^{33} \frac{[H^{\text{obs}}(z_i) - H^{\text{th}}(z_i)]^2}{\sigma_{H^{\text{obs}}(z_i)}^2}, \quad (28)$$

where $H^{\text{obs}}(z_i)$ signifies the value of the observed Hubble parameter, along with its corresponding standard deviation $\sigma_{H^{\text{obs}}(z_i)}^2$ from the table provided. The equivalent $H^{\text{th}}(z_i)$ represents the Hubble parameter value in theory obtained from the considered cosmological model.

Big Bang Nucleosynthesis (BBN): An independent method of inferring the density of baryons is to examine BBN, which serves as a probe of the early Universe's dynamics. With the help of BBN, we can look at the limitations regarding the anisotropic extensions of the conventional cosmological model [74–76]. For all of our calculations, we use an updated estimate of the physical baryon density, ω_b (where $\omega_b \equiv \Omega_b h^2$), which comes from Big Bang Nucleosynthesis (BBN) and has a value of 0.02233 ± 0.00036 . This computation makes use of revised data obtained from experimental nuclear physics at the INFN Laboratori Nazionali del Gran Sasso in Italy, at the Laboratory for Underground Nuclear Astrophysics (LUNA) [77].

Pantheon Plus and SH0ES: Historically, Type Ia supernovae (SNe Ia) have played crucial role in developing the conventional model of the universe. These supernovae yield useful distance moduli measurements, which constrain the late-time expansion rate or the uncalibrated luminosity distance $H_0 d_L(z)$. For a supernova at redshift z , the theoretical apparent magnitude m_B is determined by the following equation:

$$m_B = 5 \log_{10} \left[\frac{d_L(z)}{1 \text{Mpc}} \right] + 25 + M_B, \quad (29)$$

where M_B stands for the absolute magnitude. Consequently, the distance modulus ($\mu(z)$) can be written as $\mu(z) = m_B - M_B$. In a flat cosmology, the luminosity distance is determined as follows:

$$d_L(z) = (1+z) \int_0^z \frac{dz'}{H(z')}. \quad (30)$$

In the present study, we make use of SNe Ia distance modulus measurements from the Pantheon+ sample [78]. We name the collection as PP, which comprises 1701 light curves that correspond to 1550 unique supernovae Ia within the $z \in [0.001, 2.26]$ redshift range. We also include constraints on H_0 and M_B by including SH0ES Cepheid host distance anchors [78] into our analysis; this dataset is referred to as PPSH0ES.

We utilise PP data to minimise the equation that follows to constrain the cosmological parameters:

$$\chi_{\text{PP}}^2 = \Delta D^T C_{\text{stat+syst}}^{-1} \Delta D, \quad (31)$$

where D represents the vector of 1701 SN distance modulus residuals calculated as

$$\Delta D_i = \mu_i - \mu_{\text{model}}(z_i), \quad (32)$$

while comparing the observed supernova distance (μ_i) with the predicted model distance ($\mu_{\text{model}}(z_i)$) by utilising the measured supernova/host redshift. Here, $C_{\text{stat+syst}} = C_{\text{stat}} + C_{\text{syst}}$, with C_{stat} and C_{syst} denote the statistical and the systematic covariance matrices respectively.

While SNe analysis alone suffers from degeneracy between the parameters M_B and H_0 , we get over this restriction by adding the recently reported SH0ES Cepheid host distance anchors (R22) into the likelihood. With this change, we are able to confine M_B as well as H_0 . The following adjustments are made to the SN distance residuals after including SH0ES Cepheid host distances:

$$\Delta D'_i = \begin{cases} \mu_i - \mu_i^{\text{Cepheid}} & i \in \text{Cepheid hosts} \\ \mu_i - \mu_{\text{model}}(z_i) & \text{otherwise,} \end{cases} \quad (33)$$

where μ_i^{Cepheid} stands for the Cepheid-calibrated host-galaxy distance from SH0ES. After incorporating this data with the SH0ES Cepheid host-distance covariance matrix ($C_{\text{stat+syst}}^{\text{Cepheid}}$) from R22, the likelihood function is modified as follows:

$$\chi_{\text{PPSH0ES}}^2 = \Delta D'^T (C_{\text{stat+syst}}^{\text{SN}} + C_{\text{stat+syst}}^{\text{Cepheid}})^{-1} \Delta D',$$

where $C_{\text{stat+syst}}^{\text{SN}}$ represents the SN covariance. Further information is available in the reference [78].

The baseline free parameters of the model $w\text{CDM} + \Omega_{\sigma 0}$ and $w\text{CDM}$ are as discussed in section II. We have assumed three neutrino species, approximated as two massless states and a single massive neutrino of mass $m_\nu = 0.06 \text{ eV}$. We have used uniform priors: $\omega_b \in [0.01, 0.03]$, $\omega_c \in [0.05, 0.25]$, $H_0 \in [60, 80]$, $\Omega_{\sigma 0} \in [0, 0.001]$, $w_{\text{de}0} \in [-2, 0]$ and the publicly available Boltzmann code CLASS [79] with the parameter inference code Monte Python [80] to obtain correlated Monte Carlo Markov Chain (MCMC) samples. We analyze the MCMC samples using the python package GetDist¹.

IV. RESULTS AND DISCUSSION

In Table III, we summarize the observational constraints on free parameters and some derived parameters of the $w\text{CDM}$ and $w\text{CDM} + \Omega_{\sigma 0}$ models at 68%CL from two data combinations: BAO+CC+BBN+PP and BAO+CC+BBN+PPSH0ES. The second row over each

¹ <https://getdist.readthedocs.io/en/latest/intro.html>

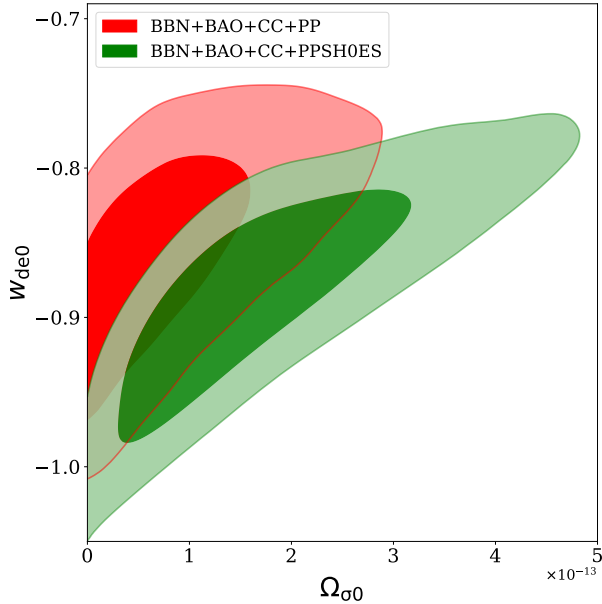


Figure 1. Two-dimensional marginalized confidence regions at 68% and 95% CL for $\Omega_{\sigma 0}$ and $w_{\text{de}0}$ for $w\text{CDM}+\Omega_{\sigma 0}$ model from BAO+CC+BBN+PP and BAO+CC+BBN+PPSH0ES data combinations.

parameter (mentioned in blue color) represents the constraints at 68%CL on ΛCDM and $\Lambda\text{CDM}+\Omega_{\sigma 0}$ models from same set of data combinations. The upper bounds on anisotropic expansion parameter, $\Omega_{\sigma 0}$, at 95% CL are of order 10^{-13} for $w\text{CDM}+\Omega_{\sigma 0}$ model with both the data combinations. The upper bounds of $\Omega_{\sigma 0}$ for this model read as: $\Omega_{\sigma 0} < 2.3 \times 10^{-13}$ and $\Omega_{\sigma 0} < 4 \times 10^{-13}$ from BAO+CC+BBN+PP and BAO+CC+BBN+PPSH0ES, respectively. On other hand, the upper bounds on anisotropic expansion parameter $\Omega_{\sigma 0}$ for $\Lambda\text{CDM}+\Omega_{\sigma 0}$ model are: $\Omega_{\sigma 0} < 2.0 \times 10^{-14}$ and $\Omega_{\sigma 0} < 6.5 \times 10^{-14}$ from BAO+CC+BBN+PP and BAO+CC+BBN+PPSH0ES combinations, respectively. Thus, we see that the $w\text{CDM}+\Omega_{\sigma 0}$ model provides weaker upper bounds on anisotropy parameter by one order of magnitude as compared to $\Lambda\text{CDM}+\Omega_{\sigma 0}$ model with both the data combinations. We observe that anisotropic parameter $\Omega_{\sigma 0}$ has a strong positive correlation with DE EoS parameter from both the data combinations. This means that larger amount of anisotropy in the Universe results larger value of DE EoS, see Figure 1.

For the $w\text{CDM}+\Omega_{\sigma 0}$ model, it can be observed from Table III that the DE EoS parameter does not prefer the cosmological constant form of DE (having $w_{\text{de}0} = -1$) with both data combinations. Also, at 95% CL, the DE EoS parameter ($w_{\text{de}0} = -0.853^{+0.096}_{-0.100}$ for BAO+CC+BBN+PP data combination and $w_{\text{de}0} = -0.88^{+0.10}_{-0.11}$ for BAO+CC+BBN+PPSH0ES data combi-

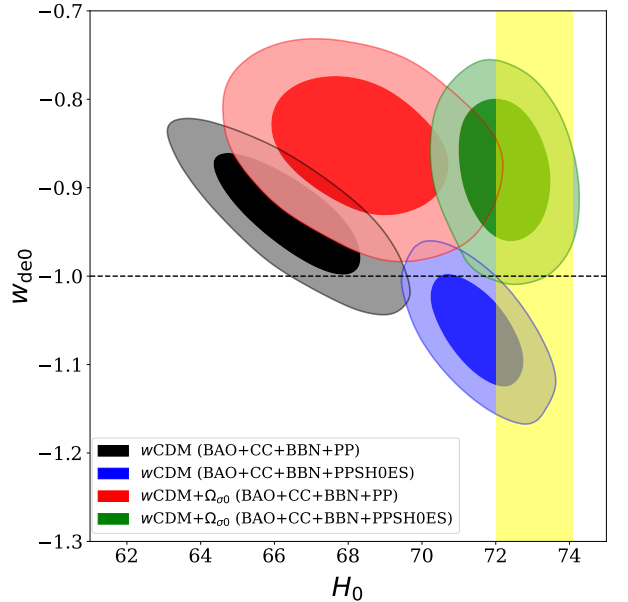


Figure 2. Two-dimensional marginalized confidence regions at 68% and 95% CL of H_0 and $w_{\text{de}0}$ for $w\text{CDM}$ and $w\text{CDM}+\Omega_{\sigma 0}$ models from BAO+CC+BBN+PP and BAO+CC+BBN+PPSH0ES data combinations. The vertical yellow band represents $H_0^{\text{R}22} = 73.04 \pm 1.04 \text{ km s}^{-1} \text{ Mpc}^{-1}$ from SH0ES measurement. The horizontal black line represents $w_{\text{de}0} = -1$.

nation) does not prefer the cosmological constant form of DE with both data combinations. For this model, the mean values of DE EoS parameter (at 68% CL as well as 95% CL range), $w_{\text{de}0}$, lie in quintessence region ($w_{\text{de}0} > -1$), pointing towards quintessence behaviour of DE with both data combinations. Also, for the $w\text{CDM}$ model, the mean value of $w_{\text{de}0}$ at 68% CL, as shown in Table III, lies in quintessence region with BAO+CC+BBN+PP data combination whereas, it touches the phantom barrier at 95% CL with the same data combination ($w_{\text{de}0} = -0.930^{+0.086}_{-0.090}$ for BAO+CC+BBN+PP data combination). Again, for the same model with BAO+CC+BBN+PPSH0ES data combination, the mean value of $w_{\text{de}0}$ lies in phantom region ($w_{\text{de}0} < -1$) at 68% CL as well as 95% CL. At 95% CL, $w_{\text{de}0} = -1.062^{+0.078}_{-0.082}$ for BAO+CC+BBN+PPSH0ES data combination. Also, we observe from Figure 2 that $w_{\text{de}0}$ finds a strong negative correlation with H_0 in case of $w\text{CDM}$ model whereas slight negative correlation in case of $w\text{CDM}+\Omega_{\sigma 0}$ model from both the data combinations.

One of the most well known and intriguing puzzle nowadays in cosmology is discrepancy between Planck CMB data within the baseline ΛCDM model and direct local measurements of the current rate of expansion of the Universe (that is, the value of Hubble constant, H_0), as discussed in Section I. Now, we discuss the constraints on Hubble constant for

Table III. Constraints at 68% CL on the free and some derived parameters of the w CDM and w CDM+ Ω_{σ_0} models from BAO+CC+BBN+PP and BAO+CC+BBN+PPSH0ES data. The upper bounds on Ω_{σ_0} at 95% CL are displayed. The Hubble constant H_0 is measured in the unit of $\text{km s}^{-1}\text{Mpc}^{-1}$. The entries in second row over each parameter (in blue colour) represent the constraints on Λ CDM and Λ CDM+ Ω_{σ_0} model parameters.

Data set	BAO+CC+BBN+PP		BAO+CC+BBN+PP+SH0ES	
Model	w CDM	w CDM+ Ω_{σ_0}	w CDM	w CDM+ Ω_{σ_0}
	Λ CDM	Λ CDM+ Ω_{σ_0}	Λ CDM	Λ CDM+ Ω_{σ_0}
$10^{-2}\omega_b$	$2.237^{+0.035}_{-0.035}$ $2.233^{+0.035}_{-0.035}$	$2.231^{+0.036}_{-0.036}$ $2.230^{+0.036}_{-0.036}$	$2.248^{+0.035}_{-0.035}$ $2.258^{+0.035}_{-0.035}$	$2.231^{+0.036}_{-0.036}$ $2.232^{+0.036}_{-0.036}$
Ω_{σ_0}	0	$< 2.3 \times 10^{-13}$ (95% CL)	0	$< 4 \times 10^{-13}$ (95% CL)
	0	$< 2.0 \times 10^{-14}$ (95% CL)	0	$< 6.5 \times 10^{-14}$ (95% CL)
w_{de0}	$-0.930^{+0.045}_{-0.045}$ -1	$-0.853^{+0.054}_{-0.048}$ -1	$-1.062^{+0.041}_{-0.041}$ -1	$-0.881^{+0.053}_{-0.053}$ -1
H_0	$66.4^{+1.3}_{-1.3}$ $68.02^{+0.84}_{-0.84}$	$68.4^{+1.6}_{-1.6}$ $70.1^{+1.2}_{-1.5}$	$71.51^{+0.83}_{-0.83}$ $70.79^{+0.69}_{-0.69}$	$72.24^{+0.82}_{-0.82}$ $72.67^{+0.85}_{-0.85}$
M_B	$-19.461^{+0.040}_{-0.040}$ $-19.418^{+0.028}_{-0.028}$	$-19.395^{+0.047}_{-0.047}$ $-19.356^{+0.039}_{-0.044}$	$-19.317^{+0.023}_{-0.023}$ $-19.330^{+0.020}_{-0.022}$	$-19.282^{+0.023}_{-0.023}$ $-19.283^{+0.024}_{-0.024}$
Ω_{m0}	$0.258^{+0.015}_{-0.015}$ $0.318^{+0.011}_{-0.011}$	$0.230^{+0.018}_{-0.018}$ $0.309^{+0.012}_{-0.012}$	$0.287^{+0.012}_{-0.012}$ $0.324^{+0.011}_{-0.011}$	$0.233^{+0.018}_{-0.018}$ $0.302^{+0.012}_{-0.012}$
z_d	$1059.3^{+1.1}_{-1.1}$ $1060.09^{+0.95}_{-0.95}$	$1058.7^{+1.1}_{-1.1}$ $1060.37^{+0.98}_{-0.98}$	$1061.99^{+0.88}_{-0.88}$ $1061.75^{+0.85}_{-0.85}$	$1059.8^{+1.1}_{-1.1}$ $1060.99^{+0.90}_{-0.90}$
r_d	$149.0^{+2.7}_{-2.7}$ $146.1^{+1.8}_{-1.8}$	$144.4^{+3.1}_{-3.1}$ $142.0^{+2.7}_{-2.7}$	$140.7^{+1.8}_{-1.8}$ $142.1^{+1.5}_{-1.5}$	$137.7^{+1.9}_{-1.9}$ $137.7^{+1.9}_{-1.9}$
χ^2_{\min}	1436.2 1438.62	1434.08 1438.58	1332.1 1334.4	1319.9 1322.94

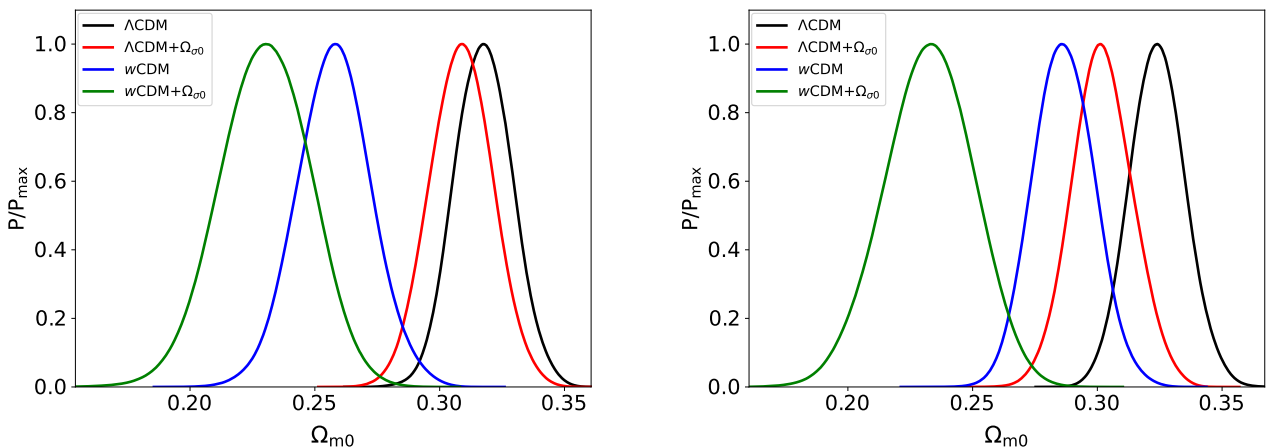


Figure 3. One-dimensional marginalized distributions of Ω_{m0} for Λ CDM, Λ CDM+ Ω_{σ_0} , w CDM and w CDM+ Ω_{σ_0} models from BAO+CC+BBN+PP (left panel) and BAO+CC+BBN+PPSH0ES (right panel) data combinations.

the considered models and compare the results with the previous work [60]. For BAO+CC+BBN+PP data combination, the constraint on H_0 for w CDM (Λ CDM) model reads: $H_0 = 66.4 \pm 1.3$ (68.02 ± 0.84) $\text{km s}^{-1}\text{Mpc}^{-1}$, and for w CDM+ Ω_{σ_0} (Λ CDM+ Ω_{σ_0}) model, it reads: $H_0 = 68.4^{+1.6}_{-1.6}$ ($70.1^{+1.2}_{-1.5}$) $\text{km s}^{-1}\text{Mpc}^{-1}$

at 68% CL. For BAO+CC+BBN+PP data combination, we have obtained lower mean values of H_0 for w CDM and w CDM+ Ω_{σ_0} models as compared to Λ CDM and Λ CDM+ Ω_{σ_0} models, respectively. For BAO+CC+BBN+PPSH0ES data combination, the constraint on H_0 for w CDM (Λ CDM) model reads: $H_0 =$

71.51 ± 0.83 (70.79 ± 0.69) $\text{km s}^{-1} \text{Mpc}^{-1}$, and for $w\text{CDM}+\Omega_{\sigma_0}$ ($\Lambda\text{CDM}+\Omega_{\sigma_0}$) model, it reads: $H_0 = 72.24 \pm 0.82$ (72.67 ± 0.85) $\text{km s}^{-1} \text{Mpc}^{-1}$ at 68% CL. Thus, from BAO+CC+BBN+PPSH0ES data $w\text{CDM}$ model provides higher mean value of H_0 as compared to ΛCDM model, whereas $w\text{CDM}+\Omega_{\sigma_0}$ and $\Lambda\text{CDM}+\Omega_{\sigma_0}$ models provide more or less the same mean values of H_0 . The highest value of Hubble constant H_0 obtained in the present analysis is 72.24 ± 0.82 $\text{km s}^{-1} \text{Mpc}^{-1}$ from BAO+CC+BBN+PPSH0ES data combinations which is consistent with $H_0^{\text{R22}} = 73.04 \pm 1.04$ $\text{km s}^{-1} \text{Mpc}^{-1}$ from SH0ES measurement. Quantifying the H_0 tension with SH0ES measurement for BAO+CC+BBN+PP data combination, we found that there is 3.9σ tension on H_0 in the $w\text{CDM}$ model and there is 2.4σ tension on H_0 in $w\text{CDM}+\Omega_{\sigma_0}$ model. Also, for BAO+CC+BBN+PPSH0ES data combination, 1.1σ tension on H_0 is observed in $w\text{CDM}$ model and 0.6σ tension is observed on H_0 in $w\text{CDM}+\Omega_{\sigma_0}$ model. So, for BAO+CC+BBN+PP data combination H_0 tension is relieved by 1.5σ in presence of anisotropy of the order 10^{-13} with constant EoS parameter of DE. Also, for BAO+CC+BBN+PPSH0ES data combination H_0 tension is relieved by 0.5σ in presence of anisotropy of the order 10^{-13} with constant EoS parameter of DE. See the Figure 2 where vertical yellow band represents $H_0^{\text{R22}} = 73.04 \pm 1.04$ $\text{km s}^{-1} \text{Mpc}^{-1}$ from SH0ES measurement and constraints on H_0 in Table III. Also, from Figure 4, we observe a positive correlation of H_0 with Ω_{σ_0} with both the data combinations. So, in order to get a larger value of H_0 , a larger amount of anisotropy is required.

Now, we discuss how $w_{\text{de}0}$ and Ω_{σ_0} affect the present day matter density parameter, $\Omega_{\text{m}0}$. Firstly, we observe that the $w\text{CDM}$ model provides significantly lower mean values of $\Omega_{\text{m}0}$ as compared to ΛCDM model for both data combinations. Second, adding anisotropy to ΛCDM model slightly reduces the mean value of $\Omega_{\text{m}0}$ for both the data combinations. Also, inclusion of anisotropy into the $w\text{CDM}$ model significantly reduces the mean values of $\Omega_{\text{m}0}$ for both the data combinations. The constraints on $\Omega_{\text{m}0}$ for $w\text{CDM}$ model are: $\Omega_{\text{m}0} = 0.258 \pm 0.015$ and $\Omega_{\text{m}0} = 0.287 \pm 0.012$ from the data combinations BAO+CC+BBN+PP and BAO+CC+BBN+PPSH0ES, respectively. The constraints on $\Omega_{\text{m}0}$ for $w\text{CDM}+\Omega_{\sigma_0}$ model are: $\Omega_{\text{m}0} = 0.230 \pm 0.018$ for the data combination BAO+CC+BBN+PP and $\Omega_{\text{m}0} = 0.233 \pm 0.018$ for the data combination BAO+CC+BBN+PPSH0ES. We can observe the deviations in the distribution of $\Omega_{\text{m}0}$ for considered models in one dimensional marginalized probability distribution as shown in Figure 3 (also, see table III) for both the data combinations. We also observe that parameters, Ω_{σ_0} and $\Omega_{\text{m}0}$ finds a negative correlation with both data combinations, see $\Omega_{\sigma_0} - \Omega_{\text{m}0}$ parametric space in the Figure 4.

The considered $w\text{CDM}$ and $w\text{CDM}+\Omega_{\sigma_0}$ models provides higher values of r_d as compared to ΛCDM and $\Lambda\text{CDM}+\Omega_{\sigma_0}$ models with BAO+CC+BBN+PP data

combination. Also, from BAO+CC+BBN+PPSH0ES data combination, we obtain the result that the $w\text{CDM}$ model prefers a lower value of r_d than ΛCDM model, but $\Lambda\text{CDM}+\Omega_{\sigma_0}$ and $w\text{CDM}+\Omega_{\sigma_0}$ provide equivalent mean values on r_d with similar error bars. Further, we notice that the addition of anisotropy reduces the value of r_d in both the cases. We can observe from Figure 4, that the parameters Ω_{σ_0} and r_d are negatively correlated with both the data combinations, which means that for a small increment in Ω_{σ_0} values, there would be corresponding decrement in r_d values.

We have observed that different model parameters are influenced due to anisotropy. For instance, we observe a negative correlation between H_0 and $w_{\text{de}0}$ which can be seen in Figure 2. Note that parameters influence each other while fitting the multi-parameter space simultaneously [81, 82]. Also, the other parameters of the models under consideration (with constant EoS of DE) are affected by anisotropy in such a way that results into the relieving of the H_0 tension up to $\sim 1\sigma$. It is important to emphasize that in equation (19), the scaling a^{-6} has relevance for the early Universe while it becomes negligible in the late Universe. Thus, the anisotropic model under consideration behaves like the Early DE model. For more about Early DE models, we refer the readers to see the recent and interesting review [33] and references therein.

V. CONCLUDING REMARKS

In the present work, we have derived CMB independent observational constraints on two simplest extensions of ΛCDM model, namely $w\text{CDM}$ and $w\text{CDM}+\Omega_{\sigma_0}$ models from recent data sets including BAO, CC, BBN, PP and PPSH0ES in two combinations: BAO+CC+BBN+PP and BAO+CC+BBN+PPSH0ES. We have obtained that DE EoS parameter favours quintessence form of DE for $w\text{CDM}+\Omega_{\sigma_0}$ model from both the data combinations at 68% CL as well as 95% CL. For the $w\text{CDM}$ model, the mean value of $w_{\text{de}0}$ at 68% CL lies in quintessence region with BAO+CC+BBN+PP data combination whereas, it touches the phantom barrier at 95% CL with the same data combination. Again, for the same model with BAO+CC+BBN+PPSH0ES data combination, the mean value of $w_{\text{de}0}$ lies in phantom region ($w_{\text{de}0} < -1$) at 95% CL. Also, we notice a strong positive correlation between $w_{\text{de}0}$ and anisotropy parameter (Ω_{σ_0}) with both data combinations, see Figure 1. The upper bounds on Ω_{σ_0} are of the order 10^{-13} from both the data combinations. The constant EoS of DE significantly affects present day matter density parameter and provides lower values for both the models (as compared to models investigated in [60] with cosmological constant DE) from both the data combinations. We have obtained higher values of Hubble constant with $H_0 = 71.51 \pm 0.83$ and $H_0 = 72.24 \pm 0.82$ $\text{km s}^{-1} \text{Mpc}^{-1}$ at 68% CL for $w\text{CDM}$ and $w\text{CDM}+\Omega_{\sigma_0}$ models, respectively with BAO+CC+BBN+PPSH0ES data. The

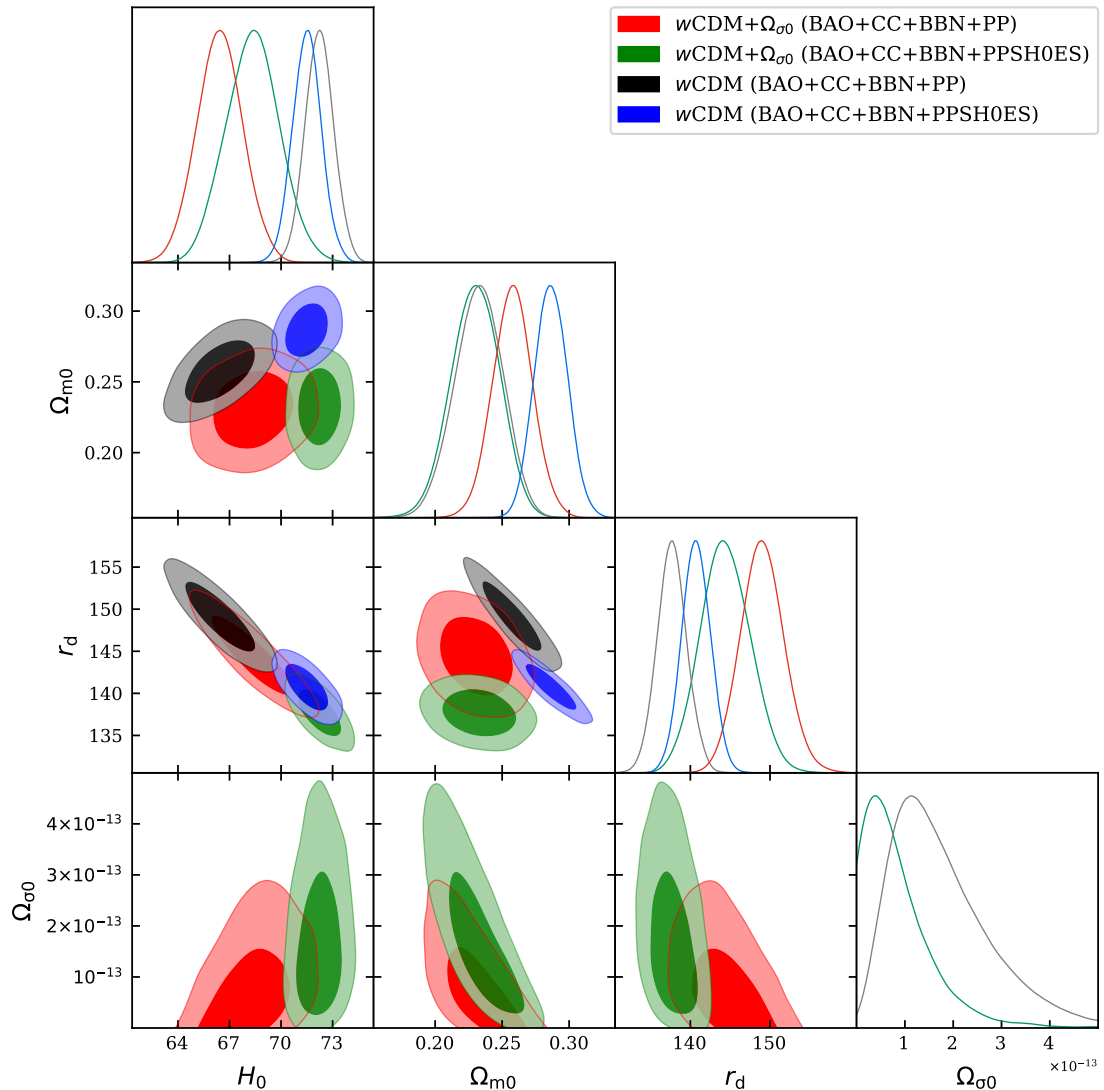


Figure 4. One and two dimensional marginalized confidence regions at 68% and 95% CL for some selected parameters of w CDM and w CDM+ $\Omega_{\sigma 0}$ models from BAO+CC+BBN+PP and BAO+CC+BBN+PPSH0ES data combinations.

obtained value of H_0 in both the considered models from BAO+CC+BBN+PPSH0ES are consistent with SH0ES measurements (H_0^{R22}), and thus H_0 tension is relieved. Further, we notice that inclusion of anisotropy parameter in the w CDM model reduces the H_0 ten-

sion by $\sim 2\sigma$ and $\sim 1\sigma$ with BAO+CC+BBN+PP and BAO+CC+BBN+PPSH0ES data combinations, respectively. Overall, we have shown that how the anisotropic extensions of standard cosmological model can influence the estimation of H_0 , and contribute significantly to the resolution of the H_0 tension.

[1] A. G. Riess *et al.* (Supernova Search Team), *Astron. J.* **116**, 1009 (1998), [arXiv:astro-ph/9805201](https://arxiv.org/abs/astro-ph/9805201).

[2] S. Perlmutter *et al.* (Supernova Cosmology Project), *Astrophys. J.* **517**, 565 (1999), [arXiv:astro-ph/9812133](https://arxiv.org/abs/astro-ph/9812133).

- [3] N. Aghanim *et al.* (Planck), *Astron. Astrophys.* **641**, A6 (2020), [Erratum: *Astron. Astrophys.* 652, C4 (2021)], arXiv:1807.06209 [astro-ph.CO].
- [4] T. M. C. Abbott *et al.* (DES), *Astrophys. J. Lett.* **872**, L30 (2019), arXiv:1811.02374 [astro-ph.CO].
- [5] M. Blomqvist *et al.*, *Astron. Astrophys.* **629**, A86 (2019), arXiv:1904.03430 [astro-ph.CO].
- [6] T. M. C. Abbott *et al.* (DES), *Phys. Rev. D* **105**, 023520 (2022), arXiv:2105.13549 [astro-ph.CO].
- [7] D. A. Riechers, A. Weiss, F. Walter, C. L. Carilli, P. Cox, R. Decarli, and R. Neri, *Nature* **602**, 58 (2022), arXiv:2202.00693 [astro-ph.GA].
- [8] E. J. Copeland, M. Sami, and S. Tsujikawa, *Int. J. Mod. Phys. D* **15**, 1753 (2006), arXiv:hep-th/0603057.
- [9] K. Bamba, S. Capozziello, S. Nojiri, and S. D. Odintsov, *Astrophys. Space Sci.* **342**, 155 (2012), arXiv:1205.3421 [gr-qc].
- [10] L. Verde, T. Treu, and A. G. Riess, *Nature Astron.* **3**, 891 (2019), arXiv:1907.10625 [astro-ph.CO].
- [11] S. J. Clark, K. Vattis, J. Fan, and S. M. Koushiappas, *Phys. Rev. D* **107**, 083527 (2023), arXiv:2110.09562 [astro-ph.CO].
- [12] A. G. Riess *et al.*, *Astrophys. J. Lett.* **934**, L7 (2022), arXiv:2112.04510 [astro-ph.CO].
- [13] W. L. Freedman, *Nature Astron.* **1**, 0121 (2017), arXiv:1706.02739 [astro-ph.CO].
- [14] E. Mörtzell and S. Dhawan, *JCAP* **09**, 025 (2018), arXiv:1801.07260 [astro-ph.CO].
- [15] L. Knox and M. Millea, *Phys. Rev. D* **101**, 043533 (2020), arXiv:1908.03663 [astro-ph.CO].
- [16] E. Di Valentino, O. Mena, S. Pan, L. Visinelli, W. Yang, A. Melchiorri, D. F. Mota, A. G. Riess, and J. Silk, *Class. Quant. Grav.* **38**, 153001 (2021), arXiv:2103.01183 [astro-ph.CO].
- [17] S. Vagnozzi, *Phys. Rev. D* **104**, 063524 (2021), arXiv:2105.10425 [astro-ph.CO].
- [18] J.-P. Hu and F.-Y. Wang, *Universe* **9**, 94 (2023), arXiv:2302.05709 [astro-ph.CO].
- [19] S. Pan, W. Yang, E. Di Valentino, E. N. Saridakis, and S. Chakraborty, *Phys. Rev. D* **100**, 103520 (2019), arXiv:1907.07540 [astro-ph.CO].
- [20] S. Kumar and R. C. Nunes, *Phys. Rev. D* **94**, 123511 (2016), arXiv:1608.02454 [astro-ph.CO].
- [21] S. Kumar and R. C. Nunes, *Phys. Rev. D* **96**, 103511 (2017), arXiv:1702.02143 [astro-ph.CO].
- [22] W. Yang, A. Mukherjee, E. Di Valentino, and S. Pan, *Phys. Rev. D* **98**, 123527 (2018), arXiv:1809.06883 [astro-ph.CO].
- [23] S. Kumar, R. C. Nunes, and S. K. Yadav, *Eur. Phys. J. C* **79**, 576 (2019), arXiv:1903.04865 [astro-ph.CO].
- [24] S. Kumar, *Phys. Dark Univ.* **33**, 100862 (2021), arXiv:2102.12902 [astro-ph.CO].
- [25] C. Kaeonikhom, H. Assadullahi, J. Schewtschenko, and D. Wands, *JCAP* **01**, 042 (2023), arXiv:2210.05363 [astro-ph.CO].
- [26] T. Bringmann, F. Kahlhoefer, K. Schmidt-Hoberg, and P. Walia, *Phys. Rev. D* **98**, 023543 (2018), arXiv:1803.03644 [astro-ph.CO].
- [27] S. Kumar, R. C. Nunes, and S. K. Yadav, *Phys. Rev. D* **98**, 043521 (2018), arXiv:1803.10229 [astro-ph.CO].
- [28] S. K. Yadav, *Mod. Phys. Lett. A* **35**, 1950358 (2019), arXiv:1907.05886 [astro-ph.CO].
- [29] V. Yadav, S. K. Yadav, and A. K. Yadav, *Phys. Dark Univ.* **42**, 101363 (2023), arXiv:2307.05155 [astro-ph.CO].
- [30] V. Poulin, T. L. Smith, T. Karwal, and M. Kamionkowski, *Phys. Rev. Lett.* **122**, 221301 (2019), arXiv:1811.04083 [astro-ph.CO].
- [31] F. Niedermann and M. S. Sloth, *Phys. Rev. D* **102**, 063527 (2020), arXiv:2006.06686 [astro-ph.CO].
- [32] J. C. Hill, E. McDonough, M. W. Toomey, and S. Alexander, *Phys. Rev. D* **102**, 043507 (2020), arXiv:2003.07355 [astro-ph.CO].
- [33] V. Poulin, T. L. Smith, and T. Karwal, *Phys. Dark Univ.* **42**, 101348 (2023), arXiv:2302.09032 [astro-ph.CO].
- [34] A. Reeves, L. Herold, S. Vagnozzi, B. D. Sherwin, and E. G. M. Ferreira, *Mon. Not. Roy. Astron. Soc.* **520**, 3688 (2023), arXiv:2207.01501 [astro-ph.CO].
- [35] O. Akarsu, J. D. Barrow, L. A. Escamilla, and J. A. Vazquez, *Phys. Rev. D* **101**, 063528 (2020), arXiv:1912.08751 [astro-ph.CO].
- [36] O. Akarsu, S. Kumar, E. Özüiker, and J. A. Vazquez, *Phys. Rev. D* **104**, 123512 (2021), arXiv:2108.09239 [astro-ph.CO].
- [37] O. Akarsu, S. Kumar, E. Özüiker, J. A. Vazquez, and A. Yadav, *Phys. Rev. D* **108**, 023513 (2023), arXiv:2211.05742 [astro-ph.CO].
- [38] O. Akarsu, E. Di Valentino, S. Kumar, R. C. Nunes, J. A. Vazquez, and A. Yadav, (2023), arXiv:2307.10899 [astro-ph.CO].
- [39] O. Akarsu, A. D. Felice, E. D. Valentino, S. Kumar, R. C. Nunes, E. Ozulker, J. A. Vazquez, and A. Yadav, “ Λ_s CDM cosmology from a type-II minimally modified gravity,” (2024), arXiv:2402.07716 [astro-ph.CO].
- [40] L. Perivolaropoulos and F. Skara, *New Astron. Rev.* **95**, 101659 (2022), arXiv:2105.05208 [astro-ph.CO].
- [41] E. Abdalla *et al.*, *JHEAp* **34**, 49 (2022), arXiv:2203.06142 [astro-ph.CO].
- [42] S. Vagnozzi, *Universe* **9**, 393 (2023), arXiv:2308.16628 [astro-ph.CO].
- [43] W. L. Freedman and B. F. Madore, *JCAP* **11**, 050 (2023), arXiv:2309.05618 [astro-ph.CO].
- [44] S. Yeung and M.-C. Chu, *Phys. Rev. D* **105**, 083508 (2022), arXiv:2201.03799 [astro-ph.CO].
- [45] J. P. Hu, Y. Y. Wang, and F. Y. Wang, *Astron. Astrophys.* **643**, A93 (2020), arXiv:2008.12439 [astro-ph.CO].
- [46] P. Fosalba and E. Gaztanaga, (2020), 10.1093/mnras/stab1193, arXiv:2011.00910 [astro-ph.CO].
- [47] P. K. Aluri *et al.*, *Class. Quant. Grav.* **40**, 094001 (2023), arXiv:2207.05765 [astro-ph.CO].
- [48] M.-a. Watanabe, S. Kanno, and J. Soda, *Phys. Rev. Lett.* **102**, 191302 (2009), arXiv:0902.2833 [hep-th].
- [49] S. Kanno, J. Soda, and M.-a. Watanabe, *JCAP* **12**, 024 (2010), arXiv:1010.5307 [hep-th].
- [50] O. Akarsu, S. Kumar, S. Sharma, and L. Tedesco, *Phys. Rev. D* **100**, 023532 (2019), arXiv:1905.06949 [astro-ph.CO].
- [51] O. Akarsu, E. Di Valentino, S. Kumar, M. Ozyigit, and S. Sharma, *Phys. Dark Univ.* **39**, 101162 (2023), arXiv:2112.07807 [astro-ph.CO].
- [52] H. Amirhashchi and S. Amirhashchi, *Phys. Rev. D* **99**, 023516 (2019), arXiv:1803.08447 [astro-ph.CO].
- [53] H. Amirhashchi and S. Amirhashchi, *Phys. Dark Univ.* **29**, 100557 (2020), arXiv:1802.04251 [astro-ph.CO].
- [54] H. Amirhashchi, A. K. Yadav, N. Ahmad, and V. Yadav, *Phys. Dark Univ.* **36**, 101043 (2022), arXiv:2001.03775 [astro-ph.CO].

- [55] A. K. Yadav, A. Alshehri, N. Ahmad, G. Goswami, and M. Kumar, *Physics of the Dark Universe* **31**, 100738 (2021).
- [56] A. K. Yadav, A. K. Yadav, M. Singh, R. Prasad, N. Ahmad, and K. P. Singh, *Physical Review D* **104**, 064044 (2021).
- [57] W. Rahman, R. Trotta, S. S. Boruah, M. J. Hudson, and D. A. van Dyk, *Mon. Not. Roy. Astron. Soc.* **514**, 139 (2022), [arXiv:2108.12497 \[astro-ph.CO\]](#).
- [58] V. K. Bhardwaj, (2023), [arXiv:2308.02864 \[gr-qc\]](#).
- [59] A. Constantin, T. R. Harvey, S. von Hausegger, and A. Lukas, *Class. Quant. Grav.* **40**, 245015 (2023), [arXiv:2212.03234 \[astro-ph.CO\]](#).
- [60] V. Yadav, *Phys. Dark Univ.* **42**, 101365 (2023), [arXiv:2306.16135 \[astro-ph.CO\]](#).
- [61] S. Alam *et al.* (eBOSS), *Phys. Rev. D* **103**, 083533 (2021), [arXiv:2007.08991 \[astro-ph.CO\]](#).
- [62] R. J. Cooke, M. Pettini, K. M. Nollett, and R. Jorgenson, *Astrophys. J.* **830**, 148 (2016), [arXiv:1607.03900 \[astro-ph.CO\]](#).
- [63] J. J. Bennett, G. Buldgen, P. F. De Salas, M. Drewes, S. Gariazzo, S. Pastor, and Y. Y. Y. Wong, *JCAP* **04**, 073 (2021), [arXiv:2012.02726 \[hep-ph\]](#).
- [64] R. Jimenez and A. Loeb, *Astrophys. J.* **573**, 37 (2002), [arXiv:astro-ph/0106145](#).
- [65] C. Zhang, H. Zhang, S. Yuan, T.-J. Zhang, and Y.-C. Sun, *Res. Astron. Astrophys.* **14**, 1221 (2014), [arXiv:1207.4541 \[astro-ph.CO\]](#).
- [66] J. Simon, L. Verde, and R. Jimenez, *Phys. Rev. D* **71**, 123001 (2005), [arXiv:astro-ph/0412269](#).
- [67] M. Moresco *et al.*, *JCAP* **08**, 006 (2012), [arXiv:1201.3609 \[astro-ph.CO\]](#).
- [68] M. Moresco, L. Pozzetti, A. Cimatti, R. Jimenez, C. Maraston, L. Verde, D. Thomas, A. Citro, R. Tojeiro, and D. Wilkinson, *JCAP* **05**, 014 (2016), [arXiv:1601.01701 \[astro-ph.CO\]](#).
- [69] A. L. Ratsimbazafy, S. I. Loubser, S. M. Crawford, C. M. Cress, B. A. Bassett, R. C. Nichol, and P. Väisänen, *Mon. Not. Roy. Astron. Soc.* **467**, 3239 (2017), [arXiv:1702.00418 \[astro-ph.CO\]](#).
- [70] D. Stern, R. Jimenez, L. Verde, M. Kamionkowski, and S. A. Stanford, *JCAP* **02**, 008 (2010), [arXiv:0907.3149 \[astro-ph.CO\]](#).
- [71] N. Borghi, M. Moresco, and A. Cimatti, *Astrophys. J. Lett.* **928**, L4 (2022), [arXiv:2110.04304 \[astro-ph.CO\]](#).
- [72] K. Jiao, N. Borghi, M. Moresco, and T.-J. Zhang, *Astrophys. J. Suppl.* **265**, 48 (2023), [arXiv:2205.05701 \[astro-ph.CO\]](#).
- [73] M. Moresco, *Mon. Not. Roy. Astron. Soc.* **450**, L16 (2015), [arXiv:1503.01116 \[astro-ph.CO\]](#).
- [74] J. P. Kneller and G. Steigman, *New J. Phys.* **6**, 117 (2004), [arXiv:astro-ph/0406320](#).
- [75] G. Steigman, *Ann. Rev. Nucl. Part. Sci.* **57**, 463 (2007), [arXiv:0712.1100 \[astro-ph\]](#).
- [76] J. D. Barrow and R. J. Scherrer, *Phys. Rev. D* **98**, 043534 (2018), [arXiv:1803.02383 \[astro-ph.CO\]](#).
- [77] V. Mossa *et al.*, *Nature* **587**, 210 (2020).
- [78] D. Brout *et al.*, *Astrophys. J.* **938**, 110 (2022), [arXiv:2202.04077 \[astro-ph.CO\]](#).
- [79] D. Blas, J. Lesgourgues, and T. Tram, *JCAP* **07**, 034 (2011), [arXiv:1104.2933 \[astro-ph.CO\]](#).
- [80] B. Audren, J. Lesgourgues, K. Benabed, and S. Prunet, *JCAP* **02**, 001 (2013), [arXiv:1210.7183 \[astro-ph.CO\]](#).
- [81] V. Marra and L. Perivolaropoulos, *Phys. Rev. D* **104**, L021303 (2021), [arXiv:2102.06012 \[astro-ph.CO\]](#).
- [82] D. Camarena and V. Marra, (2023), [arXiv:2307.02434 \[astro-ph.CO\]](#).